tigated only for the pure compound and not for dilute crystals. In the case of $K_2PbCu(NO_2)_6$, the dynamic to static transition is a long range cooperative one with the transition in the EPR caused by a crystallographic phase transition.

Although we have not yet observed a dynamic to static phase transition in the crystal structure of the copper(II) pyridine *N*-oxide species, plans are under way to examine the low-temperature crystal structure to determine if such a phenomenon will occur.

It is of interest to note that the *g* values measured from the susceptibility differ from those measured by EPR. The former is of course a macroscopic measurement, providing only the principal values of the crystal susceptibility tensor, while the latter measurements provide the microscopic or molecular values. There is therefore no inconsistency.

The major interest in the magnetic exchange interactions lies in the lower-dimensional behavior of the copper salts. Unfortunately, these phenomena are observed only below 1 K.[3,12,13] Nevertheless, the value of the exchange constant obtained here, with a very limited data set in the low-temperature region, is remarkably close to the value (-1.02 ± 0.02 K) obtained from the analysis of the data obtained below 1 K.

Registry No. $[Cu(C_5H_5NO)_6](ClO_4)_2$, 14245-15-9; $[Cu(C_5H_5NO)_6](BF_4)_2$, 23013-68-5; $[Zn(C_5H_5NO)_6](ClO_4)_2$, 23195-17-7; $[Zn(C_5H_5NO)_6](BF_4)_2$, 23013-69-6.

Supplementary Material Available: Listings of structure factor amplitudes (25 pages). Ordering information is given on any current masthead page.

References and Notes

(1) (a) University of Virginia. University of Illinois at Chicago Circle.
(2) Presented in part at the 55th Meeting of the Virginia Academy of Sciences, Petersburg, Va., 1977.
(3) C. J. O'Connor, Ph.D. Thesis, University of Illinois at Chicago Circle, 1976.
(4) C. J. O'Connor and R. L. Carlin, *Inorg. Chem.*, **14**, 291 (1975).
(5) T. J. Bergendahl and J. S. Wood, *Inorg. Chem.*, **14**, 338 (1975).
(6) A. D. van Ingen Schenau, G. C. Verschoor, and C. Romers, *Acta Crystallogr., Sect. B*, **30**, 1686 (1974).
(7) R. L. Carlin, C. J. O'Connor, and S. N. Bhatia, *J. Am. Chem. Soc.*, **98**, 685 (1976).
(8) R. L. Carlin, C. J. O'Connor, and S. N. Bhatia, *J. Am. Chem. Soc.*, **98**, 3523 (1976).
(9) J. J. Smit, L. J. de Jongh, D. De Klerk, R. L. Carlin, and C. J. O'Connor, *Physica B (Amsterdam)*, **86–88**, 1147 (1977); R. L. Carlin, C. J. O'Connor, J. J. Smit, and L. J. de Jongh, submitted for publication.
(10) H. A. Algra, L. J. deJongh, W. J. Huiskamp, and R. L. Carlin, *Physica B (Amsterdam)*, **83**, 71 (1976).
(11) K. M. Diederix, H. A. Algra, J. P. Groen, T. O. Klaassen, N. J. Poulis, and R. L. Carlin, *Phys. Lett., A*, **60**, 247 (1977); H. A. Algra, J. Bartolome, K. M. Diederix, L. J. de Jongh, and R. L. Carlin, *Physica B (Amsterdam)*, **85**, 323 (1977).
(12) H. A. Algra, L. J. de Jongh, and R. L. Carlin, to be submitted for publication.
(13) R. Navarro, H. A. Algra, L. J. de Jongh, R. L. Carlin, and C. J. O'Connor, *Physica B (Amsterdam)*, **86–88**, 693 (1977).
(14) R. L. Carlin, *J. Am. Chem. Soc.*, **83**, 3773 (1961).
(15) J. N. McElearney, D. B. Losee, S. Merchant, and R. L. Carlin, *Phys. Rev., B*, **7**, 3314 (1973).
(16) P. W. R. Corfield, R. J. Doedens, and J. A. Ibers, *Inorg. Chem.*, **6**, 197 (1967).
(17) D. T. Cromer and J. T. Waber, "International Tables for X-Ray Crystallography", Vol. IV, Kynoch Press, Birmingham, England, 1974.
(18) R. F. Stewart, E. R. Davidson, and W. T. Simpson, *J. Chem. Phys.*, **42**, 3175 (1965).
(19) D. T. Cromer and J. A. Ibers, ref 17.
(20) W. C. Hamilton, *Acta Crystallogr.*, **18**, 502 (1965).
(21) Supplementary material.
(22) J. C. Bonner and M. E. Fisher, *Phys. Rev. A*, **135**, 640 (1964).
(23) J. S. Wood and C. P. Keijzers, private communication.
(24) A. Abragam and B. Bleaney, "Electron Paramagnetic Resonance of Transition Ions", Oxford University Press, London, 1970.
(25) C. J. O'Connor, E. Sinn, and J. R. Ferraro, to be submitted for publication.
(26) D. L. Cullen and E. C. Lingafelter, *Inorg. Chem.*, **10**, 1264 (1971).
(27) B. V. Harrowfield and J. R. Pilbrow, *J. Phys. C*, **6**, 755 (1973); S. Takagi, P. G. Lenhert, and M. D. Joeston, *J. Am. Chem. Soc.*, **96**, 6606 (1974); D. Mullin, G. Heger, and D. Reinen, *Solid State Commun.*, **17**, 1249 (1975); B. V. Harrowfield, *ibid.*, **19**, 983 (1976).
(28) Y. Noda, M. Mori, and Y. Yamada, *Solid State Commun.*, **19**, 1071 (1976).

Contribution from the Ames Laboratory—Department of Energy and Department of Chemistry, Iowa State University, Ames, Iowa 50011

Synthesis and Structure of Bis(tetrapropylammonium) Tri-μ-bromo-hexabromoditungstate(2–). A Novel Odd-Electron Dimeric Anion Showing Evidence of Jahn–Teller Distortion

JOSEPH L. TEMPLETON, ROBERT A. JACOBSON, and ROBERT E. McCARLEY*

Received July 27, 1977 AIC705686

Oxidative bromination of $[(C_3H_7)_4N]^+W(CO)_5Br^-$ with 1,2-dibromoethane in refluxing chlorobenzene afforded the new compound $[(C_3H_7)_4N]_2W_2Br_9$ in high yield. Material obtained after recrystallization from acetonitrile showed simple Curie-law magnetic susceptibilities over the range 77–300 K with a magnetic moment of 1.72 μ_B. The crystals were found to be monoclinic with lattice constants $a = 36.42$ (2) Å, $b = 12.067$ (8) Å, $c = 19.62$ (1) Å, and $\beta = 95.90$ (2)°; space group $C2/c$, d(calcd) = 2.26 g cm^{-3}, d(obsd) = 2.31 g cm^{-3} with eight molecules per unit cell. Using 2255 reflections with $I \geq 3\sigma_I$ the structure was refined to $R = 0.050$ and $R_w = 0.063$. The $W_2Br_9^{2-}$ anion was found to have a confacial bioctahedral structure with d(W–W) = 2.601 (2) Å consistent with the expected W–W bond order of 2.5. An interesting distortion of the anion from D_{3h} symmetry was manifested as an effective 3° rotation of each of the planes formed by the three terminal bromine atoms on each tungsten toward the same bridging bromine atom. In this manner the real symmetry of the anion is lowered to C_{2v}. Consideration of packing effects, intramolecular nonbonded interactions, and metal–metal bonding led to the conclusion that the distortion arises from electronic effects, viz., separation of the e′ metal–metal π orbitals as dictated by the Jahn–Teller theorem.

Introduction

The study of metal–metal bonded dimeric units offers the advantage of presenting the simplest case possible for understanding attractive metal–metal interactions. In particular a large bank of data relevant to confacial bioctahedral nonahalodimetalate anions has been accumulated and analyzed.[1] Since Olsson first reported $K_3W_2Cl_9$ in 1914[2] several modifications of the general synthetic route he employed have been published.[3–5] Renewed interest in the $K_3W_2Cl_9$ species accompanied a crystal structure determination which revealed a surprisingly short W–W distance of 2.41 Å[6] as illustrated by comparison with the metal atom separation of 2.66 Å in

$Cs_3Mo_2Cl_9$.[7] Preparation of the bromide analogue of the $W_2Cl_9^{3-}$ anion has been reported twice in the chemical literature: Young synthesized $K_3W_2Br_9$ in 1932[8] via a procedure similar to that of Olsson; in 1968 Hayden and Wentworth reported insignificant yields of $W_2Br_9^{3-}$ by such methods, however, they succeeded in isolating $W_2Br_9^{3-}$ salts via the halogen exchange reaction of $W_2Cl_9^{3-}$ in concentrated hydrobromic acid.[9] No structural data related to $W_2Br_9^{3-}$ have been published, and in fact no further mention of the nonabromoditungstate(3–) anion has occurred in the literature. The one-electron oxidation of $W_2Cl_9^{3-}$ to $W_2Cl_9^{2-}$ with elemental halogen oxidants[10] confirmed the possible existence of odd-electron nonahaloditungstate anions, but no structural data have been presented.

The possible formation of metal–metal bonded dimers under mild conditions based on controlled oxidation of low-valent carbonyl-containing metal halide anions prompted considerable effort to be invested toward attaining this goal. During the course of this work, the idea of employing group 6 halocarbonylmetalates as reactants was also successfully implemented by Wentworth and co-workers.[11–13] In the work published by Wentworth the oxidation–reduction reaction between a high oxidation state metal halide and a low-valent carbonyl-containing metal species produced intermediate oxidation-state halide dimers by a conproportionation reaction. The hypothetical synthetic routes visualized for this study differed in emphasis from those of Wentworth in that no anhydrous metal halide would be required as a reactant. If one could control the reaction of carbonyl moieties with halogenation reagents to limit the final oxidation state of the metal, the precursory anhydrous metal halide preparation might be eliminated.

Wentworth and co-workers have prepared $Mo_2Cl_9^{3-,2-}$ from the redox reaction of $MoCl_6^{2-,-}$ with $Mo(CO)_4Cl_3^-$ in dichloromethane.[11] The synthetic approach they described was based upon oxidative displacement of carbon monoxide from $Mo(CO)_4Cl_3^-$ with the concomitant linking of the oxidant, either $MoCl_6^{2-}$ or $MoCl_6^-$, through the formation of halogen bridges. In later work $Mo(CO)_5X^-$ (X = Cl, Br) reacted with an appropriate metal halide ($MoCl_5$, $MoBr_4$) to produce high yields of $Mo_2Cl_9^{3-}$ and $Mo_2Br_9^{3-}$ salts.[12] The conproportionation reactions of halocarbonylmolybdates with anhydrous molybdenum halides are not paralleled by corresponding reactions in the tungsten systems. The dimeric $[(n\text{-}C_3H_7)_4N]_2[W_2Cl_9]$ species was isolated from the reaction of $W(CO)_5Cl^-$ and WCl_6,[14] but no other dimeric products were observed in similar reactions under various conditions.

In an effort to add new data to the existing pool of information related to the synthesis and properties of metal–metal bonded dimers of group 6 a new and unusual paramagnetic nonabromoditungstate anion has been synthesized and characterized. The direct synthetic route to $[(n\text{-}C_3H_7)_4N]_2[W_2Br_9]$ discovered during this investigation will be described. In addition to routine physical characterization, an x-ray structural determination was undertaken to clarify the structural details of the dimeric anion and in so doing an unusual distortion attributable to Jahn–Teller effects was revealed.

Experimental Section

Materials. Tungsten hexacarbonyl was purchased from Pressure Chemical Co. Tetrapropylammonium bromide from Eastman was purified by recrystallization from ethanol–ether solutions prior to drying under vacuum. Chlorobenzene was obtained from Fisher Scientific Co. and stored over Linde 4-A molecular sieves. Nitrogen gas was vigorously bubbled through this solvent to expel dissolved molecular oxygen prior to use. 1,2-Dibromoethane from J. T. Baker Chemical Co. was handled in the same manner as the chlorobenzene to minimize water and oxygen contamination. Acetonitrile from Fisher Scientific Co. was distilled from phosphorus pentoxide under a nitrogen atmosphere and stored in a Schlenk flask.

Synthesis. $[(n\text{-}C_3H_7)_4N][W(CO)_5Br]$ was prepared by a slightly modified version of the general preparative route described by Abel and co-workers[15] for synthesizing $M(CO)_5X^-$ anions where M = Cr, Mo, or W and X = Cl or Br. In a typical reaction the solid reactants, $W(CO)_6$ (3.52 g, 10 mmol) and $[(n\text{-}C_3H_7)_4N][Br]$ (2.66 g, 10 mmol), were loaded in a Schlenk reaction vessel equipped with a water-cooled condenser. The vessel was evacuated and then purged with nitrogen gas before 40 mL of chlorobenzene was added. The reaction flask was lowered into a heated oil bath and a rapid reaction ensued at reflux. The evolved carbon monoxide was collected for volume measurement; cessation of a continuous stream of gas signaled completion of the reaction within 15 min, at which time the golden solution of $[(n\text{-}C_3H_7)_4N][W(CO)_5Br]$ was allowed to cool to room temperature.

The second and final step in the preparative sequence was initiated by adding approximately 15 mL of 1,2-dibromoethane to the solution and heating to reflux. The solution color darkened quickly and a dark precipitate appeared within 30 min. Reflux was continued for 6 h or more to ensure expulsion of all carbon monoxide from the insoluble product. The black solid was isolated in 80–90% yields from the solution and dissolved in a minimum amount of acetonitrile to give an intense green solution. Recrystallization was effected by slow solvent removal under vacuum. Anal. Calcd for $[(n\text{-}C_3H_7)_4N]_2[W_2Br_9]$: W, 25.19; Br, 49.27; C, 19.75; H, 3.87. Found: W, 25.14; Br, 48.99; C, 19.73; H, 4.25.

Physical Measurements. Gravimetric analysis for tungsten was performed by direct ignition to the oxide, WO_3, after treating samples with concentrated nitric acid. Bromide content was determined by potentiometric titration with a standardized silver nitrate solution. Carbon and hydrogen were determined by the Ames Laboratory Analytical Services. Temperature-dependent magnetic susceptibilities were measured on a Faraday balance described previously.[16] Infrared spectra were obtained as Nujol mulls with Beckman IR-4250 and IR-11 spectrometers and electronic spectra were obtained with a Cary 14 spectrometer. Mass spectral data were obtained with an AEI 902 high-resolution mass spectrometer.

Collection and Reduction of X-Ray Data. Crystals suitable for x-ray studies were chosen from among those recrystallized from acetonitrile. Preliminary Weissenberg and precession photographs exhibited $2/m$ Laue symmetry, indicating a monoclinic space group, and needle-shaped crystals proved to have the unique b axis parallel to the needle axis. The possible space groups were Cc or $C2/c$ as evidenced by the absence of all reflections with $h + k$ odd and $h0l$ reflections with $l = 2n + 1$. A crystal of dimensions 0.05 × 0.16 × 0.35 mm was initially chosen for diffractometer data collection and wedged into a 0.2-mm Lindemann glass capillary. For reasons to be discussed later, data were also taken on a second crystal of dimensions 0.21 × 0.32 × 0.66 mm. The unit cell parameters and their standard deviations were obtained by a least-squares fit to the 2θ values of 30 independent high-angle reflections (15 from each of the two crystals) whose centers were determined by half-height counting techniques on a previously aligned four-circle diffractometer (Mo Kα radiation, λ 0.709 54 Å). The cell parameters are a = 36.42 (2) Å, b = 12.067 (8) Å, c = 19.62 (1), Å, and β = 95.90 (2)°. A calculated density of 2.26 g cm^{-3} for eight molecules per unit cell compares with the observed pycnometric density of 2.31 g cm^{-3}.

Data for both crystals were collected at room temperature using an automated four-circle diffractometer designed and built in the Ames Laboratory. The upper full circle was purchased from STOE and is equipped with encoders (Baldwin Optical) and drive motors. The design of the base allows the encoders to be directly connected to the main ω and 2θ shafts, using solid and hollow shaft encoders, respectively. The diffractometer is interfaced to a PDP-15 computer in a real-time mode and is equipped with a scintillation counter. Graphite monochromatized Mo Kα radiation was used for the data collection with a takeoff angle of 4.5°. The orientation matrix defining the relationship of the crystal lattice to the angular diffractometer settings was deduced from Polaroid exposures via an automatic indexing procedure developed by Jacobson in this laboratory.[17]

Intensity measurements for the first crystal were made using a stationary crystal–stationary counter technique after first adjusting the ω angle for each reflection to maximize its intensity. If the peak maximum did not exceed background by more than six counts, the reflection was considered unobserved. All data within a 2θ sphere of 45° ($(\sin\theta)/\lambda = 0.5$ Å^{-1}) in the hkl and $hk\bar{l}$ octants were measured in this manner for the first crystal. As a general check on electronic

and crystal stability, the intensities of three standard reflections were remeasured every 50 reflections. A scaling procedure was used to normalize the raw data based on the slight systematic decrease of the intensities observed for the three standards. Intensity data were corrected for Lorentz–polarization effects and for effects due to absorption. An absorption correction (μ = 148.4 cm^{-1}) was made using the Tompa-Alcock absorption correction program. The calculated transmission factors ranged from 0.1 to 0.4 and were in agreement with the experimentally observed variation for the 060 reflection at χ = 90.0° as a function of rotation about the ϕ axis.

Collection of data for the second crystal was performed with the same diffractometer and alignment procedure as above, but integrated intensities were measured using an ω-scan technique. All unique data in the hkl and $hk\bar{l}$ octants within a 2θ sphere of 45° were measured. Six standard reflections were remeasured after every 75 reflections as a check on crystal and instrumental stability; no significant intensity variation was observed during the data collection period. Intensity data were corrected for Lorentz–polarization and absorption effects as in the case of the first crystal. The 060 reflection was monitored as a function of ϕ at χ = 90.0°, and the observed intensity variations were consistent with calculated transmission factors ranging from 0.03 to 0.12.

The estimated error in each intensity was calculated by

$$\sigma_I^2 = C_T + C_B + (0.04C_T)^2 + (0.04C_B)^2 + (0.04C_I)^2 T_a^2$$

where C_T, C_B, C_I, and T_a are the total count, background count, net count, and the transmission factor, respectively. The estimated deviations in the structure factors were calculated by the finite-difference method.[18]

Solution and Refinement of the Structure. Solution of the structure commenced with data ($I > 3\sigma_I$) from the first crystal. A Howells, Phillips and Rodgers test indicated a centric space group; hence $C2/c$ was assumed. Analysis of a sharpened three-dimensional Patterson function[19] revealed the locations of the two independent tungsten atoms. Location of the nine bromine atoms proceeded from an electron density map phased by the tungsten atoms. A conventional discrepancy factor ($R = \sum||F_o| - |F_c||/|F_o|$) of 0.163 resulted after isotropic refinement of the thermal parameters for these 11 heavy atoms. The remaining nonhydrogen atoms were found by successive structure factor[20] and electron density map calculations.[21] These atomic positions were refined by a full-matrix least-squares procedure, minimizing the function $\sum w(|F_o| - |F_c|)^2$, where $w = 1/\sigma_F^2$. The scattering factors used were those of Hanson et al.,[22] with tungsten and bromine scattering factors modified for the real and imaginary parts of anomalous dispersion.[23] An electron density difference map verified that all the atoms had been accounted for, and anisotropic refinement of the 11 heavy atoms in the anion and isotropic refinement of the 26 light atoms in the two cations were begun. Difficulties were encountered in refining the atom parameters of the two independent tetrapropylammonium cations in the asymmetric unit. Although the basic structural conformation of the four propyl groups tetrahedrally coordinated to each of the two central nitrogen atoms was evident, the thermal parameters and interatomic distances within each cation were disturbingly variant, suggesting either excessive thermal motion not accounted for correctly by the ellipsoidal approximation or, more likely, partial disorder in the cation atomic positions. The conventional discrepancy factor had leveled off at 0.100. The tungsten and bromine atoms present in $[(n\text{-}C_3H_7)_4N]_2[W_2Br_9]$ clearly dominated the refinement and the positional coordinates and thermal parameters of these 11 heavy atoms were found to be insensitive to the location and refinement of the carbon and nitrogen atoms present in the cations. Attempts to introduce statistical disorder into the light atoms positions uniformly failed to improve the refinement.

In an effort to improve the refinement with respect to the parameters describing the light atoms, data were collected on a second crystal as described above. After data reduction, the structure factors from the second crystal were used in the calculations. Refinement of the heavy atom parameters proceeded as with the first data set, and location of the light atoms from a three-dimensional difference electron density synthesis produced results similar to those of the first data set as well. The light atom thermal parameters were large and the carbon–carbon single-bond distances varied considerably. Although the two data sets were collected for crystals of different size and selected from different preparations, and different data collection techniques were employed, the results of the two independent determinations were basically the same. This observation indicated that averaging the two data sets for use in the final refinement cycles would be justified as a means of eliminating any systematic errors present in either the data collection techniques or the absorption computations. Structure factors with symmetry equivalent indices that deviated by more than 20% from the average structure factor value of the two data points were considered suspect and hence were discarded. Of the 2370 equivalent reflections in the two data sets with $I \geq 3\sigma_I$, 2255 agreed sufficiently well for use in the final refinement. Most of the reflections discarded fell in the high 2θ range.

A satisfactory discrepancy factor was obtained with the averaged data set. Anisotropic refinement of all nonhydrogen atoms led to R = 0.050 and $R_w = [\sum w(|F_o| - |F_c|)^2/\sum w(F_o)^2]^{1/2}$ = 0.063. Statistical analysis of $w\Delta^2$, where $\Delta = ||F_o| - |F_c||$, as a function of the scattering angle and magnitude of F_o revealed no unusual trends and suggested that the weighting scheme was reasonable. Although a significant improvement in the discrepancy factor had been realized, little change was evident in the cation parameters. In any case the structural results of importance are the parameters which describe the anion and we have demonstrated that these are not significantly affected by the light atom parameters. The final positional and thermal parameters are listed in Table I. The standard deviations were calculated from the inverse matrix of the final least-squares cycle.[24] A final electron density difference map revealed only a peak of 3.5 e Å^{-3} located in the region between the two tungsten atoms and the three bridging bromine atoms. This residual electron density was attributed to cumulative Fourier series termination errors associated with the nearby heavy atoms as no extinction effects were evident in the data.

Tables of observed and calculated structure factor amplitudes for this structure are available as supplementary material.

Results and Discussion

Synthesis of $[(n\text{-}C_3H_7)_4N]_2W_2Br_9$. The majority of preparative reactions which form metal–metal bonded metal halides are either reductions of high oxidation state halides or disproportionations of intermediate oxidation states.[25] Direct oxidation of elemental metals with halogenating agents has only rarely been a method of choice for producing metal–metal bonded compounds. Consideration of the chemical properties deemed most important in likely reactants suggested that metal carbonyl species could be profitably employed in preparing low-valent metal halides and perhaps replace the more common high-temperature, sealed tube techniques in some instances. The synthetic basis for these reactions was to take advantage of the increased lability of carbon monoxide which accompanies oxidation of the metal to expel the carbonyl ligands under reflux at an appropriate temperature. The concept of producing reactive metal halide intermediates by thermal displacement of carbon monoxide ligands and thereby lowering coordination number would seem to be a well-founded approach to promoting metal–metal attractions. The use of a noncoordinating solvent is dictated in order to avoid the formation of monomeric metal halide adducts. This synthetic philosophy prompted considerable effort to be expended in hopes of isolating tractable products from reactions implementing the above concepts.

A cursory exploration of the reaction between tungsten hexacarbonyl and tetrapropylammonium bromide in refluxing 1,2-dibromoethane led to a dark solution with gas evolution proceeding far beyond the amount corresponding to the loss of one carbonyl per tungsten. The excess gas evolution clearly indicated that the reaction had passed beyond the expected $W(CO)_5Br^-$, and the reaction solution was allowed to reflux overnight. The insoluble black solid which resulted displayed a clean, but not bright, green color after grinding. The infrared spectrum in the region from 700 to 4000 cm^{-1} confirmed the presence of tetrapropylammonium cations and the absence of carbon monoxide ligands in the solid product. Preliminary analyses indicated the formulation $[(n\text{-}C_3H_7)_4N]_2[W_2Br_9]$ was deserving of further investigation. From a mass balance analysis of reactants and product it became clear that 1,2-dibromoethane served as a source of bromine in the reaction.

Table I

Final Positional Parameters for $[(n\text{-}C_3H_7)_4N]_2[W_2Br_9]$[a]

Atom	x	y	z	Atom	x	y	z
W(1)	0.38141 (3)	0.3262 (1)	0.3840 (1)	C(7)	0.396 (1)	0.239 (5)	0.020 (2)
W(2)	0.36504 (3)	0.1425 (1)	0.3184 (1)	C(8)	0.365 (2)	0.199 (6)	−0.020 (3)
Br(1)	0.3906 (1)	0.5079 (3)	0.3232 (1)	C(9)	0.331 (1)	0.195 (3)	−0.022 (2)
Br(2)	0.3437 (1)	0.4255 (3)	0.4671 (1)	C(10)	0.453 (1)	0.256 (7)	−0.033 (3)
Br(3)	0.4389 (1)	0.3544 (3)	0.4670 (1)	C(11)	0.452 (2)	0.289 (6)	−0.087 (2)
Br(4)	0.3082 (1)	0.0211 (3)	0.3241 (2)	C(12)	0.475 (1)	0.287 (3)	−0.141 (2)
Br(5)	0.3566 (1)	0.1305 (3)	0.1893 (1)	C(13)	0.205 (1)	0.265 (4)	0.395 (2)
Br(6)	0.4047 (1)	−0.0281 (3)	0.3290 (1)	C(14)	0.210 (1)	0.384 (4)	0.397 (2)
Br(7)	0.3191 (1)	0.3089 (2)	0.3072 (1)	C(15)	0.228 (1)	0.435 (2)	0.457 (2)
Br(8)	0.4269 (1)	0.2429 (3)	0.3041 (1)	C(16)	0.185 (1)	0.088 (3)	0.356 (2)
Br(9)	0.3707 (1)	0.1455 (2)	0.4515 (1)	C(17)	0.207 (1)	0.005 (4)	0.357 (2)
N(1)	0.4374 (8)	0.247 (2)	0.032 (1)	C(18)	0.205 (1)	−0.103 (3)	0.395 (1)
N(2)	0.1861 (6)	0.206 (2)	0.330 (1)	C(19)	0.149 (1)	0.259 (4)	0.306 (2)
C(1)	0.444 (1)	0.355 (3)	0.076 (2)	C(20)	0.124 (1)	0.277 (4)	0.356 (2)
C(2)	0.449 (2)	0.385 (5)	0.132 (2)	C(21)	0.086 (1)	0.295 (4)	0.331 (2)
C(3)	0.458 (1)	0.482 (3)	0.170 (2)	C(22)	0.212 (1)	0.216 (3)	0.269 (2)
C(4)	0.447 (2)	0.143 (4)	0.074 (5)	C(23)	0.201 (1)	0.158 (3)	0.205 (2)
C(5)	0.480 (2)	0.131 (5)	0.110 (6)	C(24)	0.231 (1)	0.157 (3)	0.157 (1)
C(6)	0.486 (1)	0.023 (4)	0.154 (3)				

Final Thermal Parameters ($\times 10^3$) for $[(n\text{-}C_3H_7)_4N]_2[W_2Br_9]$[b]

Atom	β_{11}	β_{22}	β_{33}	β_{12}	β_{13}	β_{23}
W(1)	1.04 (1)	9.3 (1)	2.96 (1)	0.10 (3)	0.32 (1)	0.12 (5)
W(2)	1.12 (1)	8.6 (1)	2.97 (3)	0.08 (3)	0.40 (1)	0.17 (5)
Br(1)	1.58 (3)	11.7 (3)	5.4 (1)	−0.44 (9)	0.21 (5)	2.2 (1)
Br(2)	1.97 (4)	13.2 (3)	4.7 (1)	0.9 (1)	1.19 (6)	−0.8 (1)
Br(3)	1.46 (3)	16.7 (4)	5.1 (1)	0.2 (1)	−0.59 (5)	−0.4 (2)
Br(4)	1.43 (3)	12.4 (3)	6.1 (1)	−0.80 (9)	0.38 (6)	1.3 (1)
Br(5)	1.92 (4)	14.2 (3)	3.2 (1)	−0.2 (1)	0.13 (5)	−0.1 (1)
Br(6)	1.84 (4)	12.5 (3)	5.3 (1)	1.6 (1)	0.55 (6)	0.4 (1)
Br(7)	1.12 (3)	10.6 (3)	5.5 (1)	0.35 (8)	−0.23 (5)	−0.1 (1)
Br(8)	1.25 (3)	14.9 (3)	5.1 (1)	−0.21 (9)	1.00 (5)	−0.8 (1)
Br(9)	2.27 (4)	11.0 (3)	3.0 (1)	−0.2 (1)	0.67 (5)	0.5 (1)
N(1)	1.8 (2)	6.7	8.8	−1.0	1.7	−3.9
N(2)	1.0 (2)	17.2	2.3	−0.6	0.3	−0.5
C(1)	4.3 (9)	15 (4)	7 (2)	−1.8	0.1	−2.3
C(2)	10 (2)	30 (8)	6 (1)	1.6	4.1	−7.6
C(3)	3.1 (6)	18 (4)	8 (2)	−4.1	1.6	−3.7
C(4)	3 (1)	8 (4)	26 (6)	2.4	0.5	−1.0
C(5)	4 (1)	21 (8)	27 (8)	1.9	−1.2	4.9
C(6)	3.3 (8)	19 (5)	15 (3)	1.2	2.6	6.5
C(7)	2.8 (6)	5 (1)	4 (1)	−6.7	1.4	−0.8
C(8)	4 (1)	4 (1)	7 (2)	4.9	−2.2	−3.7
C(9)	1.3 (3)	23 (6)	7 (1)	−0.8	−1.5	−0.4
C(10)	2.5 (6)	8 (1)	8 (2)	−6.5	0.6	10.0
C(11)	5 (1)	4 (1)	3 (1)	−4.9	2.5	−1.2
C(12)	1.7 (4)	24 (5)	6 (1)	0.7	0.7	0.1
C(13)	1.8 (5)	20 (5)	9 (2)	−0.3	−0.3	−7.0
C(14)	2.3 (6)	15 (5)	10 (2)	0.2	−0.1	−2.1
C(15)	2.8 (5)	10 (3)	6 (1)	−0.7	−0.3	−1.9
C(16)	5.6 (9)	17 (5)	5 (1)	2.7	4.5	4.5
C(17)	3.7 (7)	20 (6)	8 (1)	3.0	3.7	2.9
C(18)	2.2 (4)	14 (3)	4 (1)	−1.9	−0.2	1.9
C(19)	0.9 (3)	37 (7)	8 (2)	−0.1	0.0	−5.8
C(20)	1.1 (3)	38 (7)	10 (2)	3.2	0.2	−6.1
C(21)	1.8 (4)	26 (5)	10 (2)	2.1	2.6	5.5
C(22)	3.8 (7)	12 (3)	7 (1)	−2.7	0.2	−1.5
C(23)	3.7 (8)	9 (4)	10 (2)	−0.4	0.0	2.9
C(24)	2.2 (4)	19 (5)	5 (1)	0.3	2.0	−1.3

[a] Numbers in parentheses are the estimated standard deviations of the coordinates and refer to the last significant digit of the preceding number. [b] The form of the anisotropic temperature factor expression is $\exp[-(\beta_{11}h^2 + \beta_{22}k^2 + \beta_{33}l^2 + 2\beta_{12}hk + 2\beta_{13}hl + 2\beta_{23}kl)]$.

A second preparation of this same product was carried out using chlorobenzene as a solvent to cleanly form the $W(CO)_5Br^-$ anion prior to adding excess 1,2-dibromoethane as the oxidant as expressed in eq 1 and 2. A red solution was

$$[(n\text{-}C_3H_7)_4N][Br] + W(CO)_6 \rightarrow [(n\text{-}C_3H_7)_4N][W(CO)_5Br] + CO(g) \quad (1)$$

$$4[(n\text{-}C_3H_7)_4N][W(CO)_5Br] + 7C_2H_4Br_2 \rightarrow 2[(n\text{-}C_3H_7)_4N]_2[W_2Br_9] + 7C_2H_4(g) + 20CO(g) \quad (2)$$

evident at reflux, but when cooled the solution assumed a light brown color similar in appearance to weak tea. The black, microcrystalline precipitate smeared to the green color observed previously, and quantitative analyses for W, Br, C, and H were in excellent agreement with the calculated values for $[(n\text{-}C_3H_7)_4N]_2[W_2Br_9]$. Yields of 80–90% were consistently obtained when the synthesis was repeated. The product was extremely soluble in acetonitrile, and large crystals were obtained by recrystallization from dark green acetonitrile solutions via slow solvent removal under vacuum.

A possible reaction mechanism for the oxidation of the tungsten carbonyl species is suggested by the reaction of vicinal

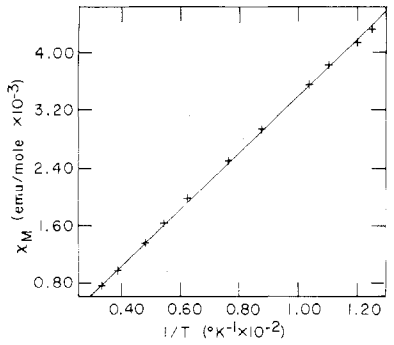

Figure 1. Curie plot (χ_M vs. T^{-1}) for $[(C_3H_7)_4N]_2[W_2Br_9]$. Straight line represents best least-squares fit to the data.

dihalides with metallic zinc to generate alkenes. Assuming ethylene results from the reduction of 1,2-dibromoethane, a balanced equation for the redox reaction can be written as shown in eq 2. Identification of ethylene in the gaseous reaction products was possible via high-resolution mass spectral analysis. An evacuated flask was placed in the exhaust line of the reaction vessel by means of a T joint, and after addition of the dibromoethane and 10 min of vigorous reflux the flask was opened to collect a sample of the evolved gas. The reaction was performed as usual under a nitrogen atmosphere, and hence all three of the gaseous species present have a mass near 28 amu (CO, 27.995; N_2, 28.006; C_2H_4, 28.031), but a high-resolution mass spectrum clearly indicated the presence of appreciable quantities of ethylene. Thus, the proposed reaction equation was satisfactorily confirmed.

Several points deserve emphasis in considering the advantages relating to the synthetic route described for preparing this dimeric compound. First of all no high oxidation state anhydrous metal halide is required as a reactant. Second, the reagents are commercially available, easily handled, and inexpensive. Third, the entire preparation can be conveniently completed in 1 day, and, finally, good yields are reproducibly obtained.

Physical Characterizations of $[(n\text{-}C_3H_7)_4N]_2[W_2Br_9]$. The dimeric formulation $[(n\text{-}C_3H_7)_4N]_2[W_2Br_9]$ requires the presence of at least one unpaired electron in the ground state. The magnetic behavior of this compound was examined via a temperature-dependent magnetic susceptibility study between liquid nitrogen and room temperature. Eleven temperatures were selected at roughly equal intervals in terms of $1/T$ and forces were measured at each of five magnetic field strengths on a sample which had been recrystallized from acetonitrile. The plot of χ_M vs. $1/T$ was linear as shown in Figure 1 and the Curie formulation was employed as expressed in eq 3 where

$$\chi_M = C/T + \chi_D + \chi_{TIP} \quad (3)$$

χ_M is the molar susceptibility, χ_D is the diamagnetic contribution due to the presence of paired electrons, χ_{TIP} is the temperature-independent paramagnetic contribution, and $C = N\beta^2\mu^2/3k$. A least-squares fit to the 11 data points confirmed the linear $1/T$ dependence as evidenced by the values shown in eq 4. The values of the magnetic moment and the

$$\chi_M = (0.370 \pm 0.002 \text{ K emu/mol})(1/T) - (452 \pm 19) \times 10^{-6} \text{ emu/mol} \quad (4)$$

temperature-independent paramagnetic contribution were calculated from the values of the slope and intercept to be 1.72 μ_B and 247 × 10^{-6} emu/mol, respectively. The magnetic moment is entirely consistent with a single unpaired electron in the ground state and compares favorably with the theoretical spin-only moment of 1.73 μ_B. The temperature-independent paramagnetic contribution, calculated from a value of −699 × 10^{-6} emu/mol for the diamagnetic contribution, was not unexpected in view of a similar value of 193 × 10^{-6} emu/mol reported for the metal–metal bonded dimer $Nb_2Cl_6(SC_4H_8)_3$.[26] At 298 K the value of μ_{eff}, which includes the contribution from χ_{TIP}, is computed as 2.88 μ_B; this is in excellent agreement with the value of 2.87 μ_B reported for $(Bu_4N)_2W_2Cl_9$.[10]

Infrared data in the region from 700 to 4000 cm^{-1} established the presence of tetrapropylammonium cations in the product by comparison with tetrapropylammonium bromide infrared data. In addition, the absence of carbonyl ligands was definitely established by the absence of absorptions between 1600 and 2600 cm^{-1}.

The low-frequency region of the infrared spectrum was dominated by two principal absorptions at 232 and 208 cm^{-1}. These very strong bands were assigned to terminal metal–halogen stretching modes of symmetries A_2'' and E′, respectively, because of the obvious parallels with similar assignments in a normal-coordinate analysis of $M_2X_9^{3-}$ compounds by Ziegler and Risen.[27] These assignments assume the $W_2Br_9^{2-}$ anion conforms to the D_{3h} symmetry of a confacial bioctahedral dimer, as confirmed by the structural determination discussed below. The above two symmetry modes are infrared allowed while the remaining terminal vibrations of A′ and E″ symmetry representations in this D_{3h} group are not allowed.

Some comparable metal–chloride terminal vibrational frequencies are listed in Table II for various $M_2Cl_9^{2-,3-}$ anions. Particularly relevant to this work is the dependence of the observed intensity of the $W_2Cl_9^{3-}$ anion vibrations on the cation present in the lattice. Only the tetraalkylammonium cations have provided very strong bands for both the A_2'' and E′ terminal modes. Furthermore, the other low-frequency vibrations in $[(n\text{-}C_4H_9)_4N]_3[W_2Cl_9]$ were reported of only moderate intensity or less relative to the two very intense absorptions mentioned above;[27] such a spectrum is consistent with the present observation of only two strong bands in $[(n\text{-}C_3H_7)_4N]_2[W_2Br_9]$.

One can legitimately compare $M_2Cl_9^{n-}$ vibrational frequencies with those of $M_2Br_9^{n-}$ as a function of the halide mass ratio only when the value of n remains unchanged. The sensitivity of infrared band locations to the oxidation state of the metal invalidates a comparison of $W_2Br_9^{2-}$ and $W_2Cl_9^{3-}$ metal–halogen frequencies on a mass basis alone. A better gauge is to note that it is common for isoelectronic compounds of the second- and third-row group 6 metals to display metal–halogen stretching modes of nearly identical frequencies, i.e., $Mo_2Cl_9^{3-}$ and $W_2Cl_9^{3-}$. If one assumes a confacial bioctahedral structure for $W_2Br_9^{2-}$ with metal–halogen force constants producing frequencies related to those of $Mo_2Cl_9^{2-}$ by the square root of the halogen mass ratio, one calculates expected frequencies of 230 and 203 cm^{-1} for the terminal A_2'' and E′ vibrations of $W_2Br_9^{2-}$, respectively, and both agree well with the observed energies of 232 and 208 cm^{-1}.

A solution electronic spectrum of $[(n\text{-}C_3H_7)_4N]_2[W_2Br_9]$ was obtained in acetonitrile. The frequencies of the observed band maxima (10^3 cm^{-1}) and estimates of the corresponding

Table II. Low-Frequency Metal–Halogen Vibrations in $M_2X_9^{n-}$

Compd	Terminal metal–halogen vibrational modes,[a] cm^{-1} A_2''	E′
$[(n\text{-}C_3H_7)_4N]_3Mo_2Cl_9$[b]	318 s	290 s
$[(n\text{-}C_4H_9)_4N]_2Mo_2Cl_9$[b]	345 s	305 s
$Cs_3W_2Cl_9$[c]	313 vs	282 w
$K_3W_2Cl_9$[c]	313 vs	285 w
$[(n\text{-}C_4H_9)_4N]_3W_2Cl_9$[c]	311 vs	289 vs
$[(n\text{-}C_3H_7)_4N]_2W_2Br_9$[d]	232 vs	208 vs

[a] All data were obtained on Nujol mulls. Abbreviations: s, strong; w, weak; v, very. [b] Data from ref 13. [c] Data from ref 27. [d] This work.

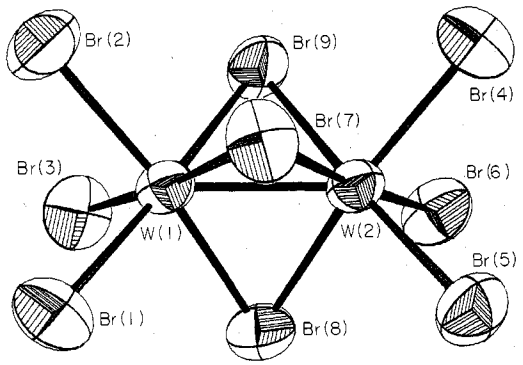

Figure 2. A view of the anion $W_2Br_9^{2-}$ in $[(C_3H_7)_4N]_2[W_2Br_9]$ showing 50% probability ellipsoids and the atomic labeling scheme.

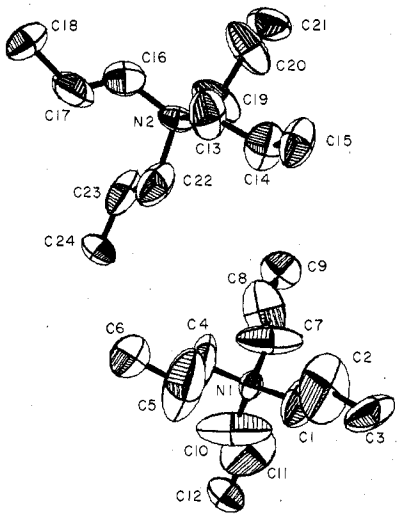

Figure 3. A view of the two independent cations $[(C_3H_7)_4N]^+$ in $[(C_3H_7)_4N]_2[W_2Br_9]$ showing the 33% probability ellipsoids and the atomic labeling scheme.

extinction coefficients (M^{-1} cm^{-1}) follow: 13.0 (1100), 16.1 (1300), 18.2 (1100), 23.8 (5100), and 27.0 (6600). The large extinction coefficients reported here for the nonabromoditungstate(2–) anion are similar in magnitude to those published for $W_2Cl_9^{2-}$ in dichloromethane: 1040 and 1700 M^{-1} cm^{-1} for bands at 1.353 and 1.720 μm^{-1}, respectively.[10]

Description of the Structure. The confacial bioctahedral structure of the nonabromoditungstate(2–) anion is illustrated in Figure 2, and the two independent cation conformations are shown in Figure 3. Bond lengths, bond angles, and significant nonbonded distances within the $W_2Br_9^{2-}$ anion are listed in Table III, while the bond distances found for the tetrapropylammonium cation are presented in Table IV. The structure is best described as two octahedra sharing a common face such as has been observed for $M_2X_9^{3-}$ salts structurally characterized by other workers.[1]

The W–W distance of 2.601 (2) Å in $W_2Br_9^{2-}$ is definitely in the range of strong metal–metal attractive forces, even though it is 0.19 Å longer than the corresponding distance in $W_2Cl_9^{3-}$ (2.41 Å).[6] Distortional moduli derived for confacial bioctahedral structures which retain D_{3h} symmetry while undergoing contraction or elongation along the metal–metal axis were introduced by Cotton and Ucko,[1] and their application here seems necessary to correctly assess the extent of the metal–metal interaction. A comparison of the generalized parameter values for $W_2Br_9^{2-}$ ($d'/d'' = 0.90$, $90.0° - \alpha' = -7.1°$, and $\beta - 70.5° = -10.5°$) with those of other group 6 confacial bioctahedral dimers is tabulated in Table V. The definitions of d′, d″, α', and β are as given by Cotton and Ucko and illustrated for the general case in Figure 4. The moduli cited above serve to illustrate the nature and degree of distortion from the idealized confacial bioctahedron formed from two congruent octahedra, due to metal–metal attraction or repulsion. The two tungsten dimers, $K_3W_2Cl_9$ and $[(n\text{-}C_3H_7)_4N]_2[W_2Br_9]$, are clearly separated from the other dimers by greater axial distortions due to contraction as re-

Table III. Bond Distances (Å), Nonbonded Distances (Å), and Angles (deg) in $W_2Br_9^{2-}$

Bond Distances			
W(1)–W(2)	2.601 (2)	W(1)–Br(7)	2.600 (3)
W(1)–Br(1)	2.535 (4)	W(1)–Br(8)	2.597 (4)
W(1)–Br(2)	2.538 (4)	W(1)–Br(9)	2.602 (4)
W(1)–Br(3)	2.544 (4)	W(2)–Br(7)	2.608 (4)
W(2)–Br(4)	2.547 (4)	W(2)–Br(8)	2.597 (4)
W(2)–Br(5)	2.525 (4)	W(2)–Br(9)	2.599 (4)
W(2)–Br(6)	2.514 (4)	Av W–Br_b[a]	2.601
Av W–Br_t[a]	2.534		
Nonbonded Distances			
Br(1)–Br(2)	3.588 (5)	Br(1)–Br(7)	3.535 (5)
Br(1)–Br(3)	3.671 (5)	Br(1)–Br(8)	3.494 (6)
Br(2)–Br(3)	3.574 (6)	Br(2)–Br(7)	3.472 (5)
Br(4)–Br(5)	3.579 (5)	Br(2)–Br(9)	3.542 (5)
Br(4)–Br(6)	3.558 (6)	Br(3)–Br(8)	3.456 (5)
Br(5)–Br(6)	3.643 (5)	Br(3)–Br(9)	3.531 (6)
Av Br_t–Br_t	3.602	Br(4)–Br(7)	3.515 (6)
Br(7)–Br(8)	4.011 (5)	Br(4)–Br(9)	3.537 (5)
Br(7)–Br(9)	3.788 (5)	Br(5)–Br(7)	3.535 (5)
Br(8)–Br(9)	3.891 (5)	Br(5)–Br(8)	3.504 (5)
Av Br_b–Br_b	3.897	Br(6)–Br(8)	3.416 (6)
		Br(6)–Br(9)	3.509 (5)
		Av Br_t–Br_b	3.504
Angles			
W(1)–Br(7)–W(2)	59.93 (8)	Br(1)–W(1)–Br(7)	87.0 (1)
W(1)–Br(8)–W(2)	60.10 (9)	Br(1)–W(1)–Br(8)	85.8 (1)
W(1)–Br(9)–W(2)	60.02 (8)	Br(2)–W(1)–Br(7)	85.0 (1)
Av W–Br_b–W	60.02	Br(2)–W(1)–Br(9)	87.1 (1)
Br(7)–W(1)–Br(8)	101.1 (1)	Br(3)–W(1)–Br(8)	84.5 (1)
Br(7)–W(1)–Br(9)	93.5 (1)	Br(3)–W(1)–Br(9)	86.7 (1)
Br(8)–W(1)–Br(9)	96.9 (1)	Br(4)–W(2)–Br(7)	86.0 (1)
Br(7)–W(2)–Br(8)	100.8 (1)	Br(4)–W(2)–Br(9)	86.8 (1)
Br(7)–W(2)–Br(9)	93.4 (1)	Br(5)–W(2)–Br(7)	87.0 (1)
Br(8)–W(2)–Br(9)	97.0 (1)	Br(5)–W(2)–Br(8)	86.3 (1)
Av Br_b–W–Br_b	97.1	Br(6)–W(2)–Br(8)	83.9 (1)
Br(1)–W(1)–Br(2)	90.0 (1)	Br(6)–W(2)–Br(9)	86.7 (1)
Br(1)–W(1)–Br(3)	92.6 (1)	Av $(Br_t\text{–}W\text{–}Br_b)_{cis}$	86.1
Br(2)–W(1)–Br(3)	89.4 (1)	Br(1)–W(1)–Br(9)	177.1 (1)
Br(4)–W(2)–Br(5)	89.8 (1)	Br(2)–W(1)–Br(8)	172.4 (1)
Br(4)–W(2)–Br(6)	89.3 (1)	Br(3)–W(1)–Br(7)	174.4 (1)
Br(5)–W(2)–Br(6)	92.6 (1)	Br(4)–W(2)–Br(8)	172.0 (1)
Av Br_t–W–Br_t	90.6	Br(5)–W(2)–Br(9)	176.5 (1)
		Br(6)–W(2)–Br(7)	175.3 (1)
		Av $(Br_t\text{–}W\text{–}Br_b)_{trans}$	174.6

[a] Subscript abbreviations: t = terminal, b = bridge.

Table IV. Bond Distances (Å) in the Tetrapropylammonium Cations of $[(n\text{-}C_3H_7)_4N]_2[W_2Br_9]$

Cation No. 1			
N(1)–C(1)	1.57 (5)	C(1)–C(2)	1.16 (6)
N(1)–C(4)	1.54 (7)	C(2)–C(3)	1.41 (7)
N(1)–C(7)	1.47 (5)	C(4)–C(5)	1.33 (9)
N(1)–C(10)	1.47 (6)	C(5)–C(6)	1.57 (8)
Av N(1)–C	1.51	C(7)–C(8)	1.40 (7)
		C(8)–C(9)	1.25 (8)
		C(10)–C(11)	1.13 (6)
		C(11)–C(12)	1.43 (6)
		Av C–C	1.34
Cation No. 2			
N(2)–C(13)	1.56 (4)	C(13)–C(14)	1.45 (6)
N(2)–C(16)	1.52 (5)	C(14)–C(15)	1.43 (5)
N(2)–C(19)	1.52 (4)	C(16)–C(17)	1.28 (6)
N(2)–C(22)	1.61 (5)	C(17)–C(18)	1.52 (5)
Av N(2)–C	1.55	C(19)–C(20)	1.41 (6)
		C(20)–C(21)	1.45 (5)
		C(22)–C(23)	1.46 (6)
		C(23)–C(24)	1.52 (6)
		Av C–C	1.44

Table V. Selected Confacial Bioctahedral Structural Comparisons[a]

Modulus	$W_2Br_9^{2-}$ [b]	$W_2Cl_9^{3-}$	$Mo_2Br_9^{3-}$	$Mo_2Cl_9^{3-}$	$Cr_2Br_9^{3-}$	$Cr_2Cl_9^{3-}$	$Mo_2Cl_8H^{3-}$ [c]
M-M, Å	2.60	2.41	2.82	2.66	3.32	3.12	2.38
X_{br}-M-X_{br}, α', deg	97.1	98	93.9	94.2	83.0	85.8	99.2
M-X_{br}-M, β, deg	60.0	58	64.9	64.5	80.0	76.4	56.8
d'/d''	0.90	0.90	0.97	0.98	1.28	1.23	0.89
90.0° − α', deg	−7.1	−8	−3.9	−4.2	7.0	4.2	−9.2
β − 70.5°, deg	−10.5	−12.5	−5.6	−6.0	9.5	5.9	−13.7

[a] Data taken from ref 1 unless otherwise noted. [b] This work. [c] Structural data were initially reported for the compound $Rb_3Mo_2Cl_8$ (M. J. Bennett, J. V. Brencic, and F. A. Cotton, *Inorg. Chem.*, 8, 1060 (1969)), but subsequent work has established that the compound is correctly formulated as $Rb_3Mo_2Cl_8H$ (F. A. Cotton and B. J. Kalbacher, *Inorg. Chem.*, **15**, 522 (1976)).

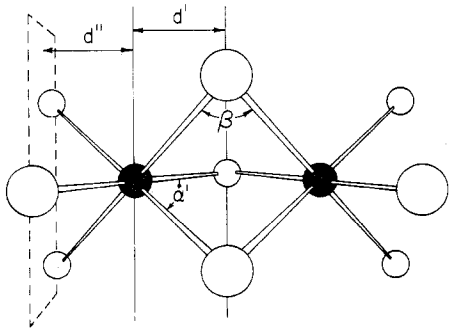

Figure 4. A general illustration of the confacial bioctahedral parameters d', d'', α', and β.

flected in the numerical values of the moduli proposed by Cotton and Ucko.

The similarity of the distortional parameter value calculated for $W_2Br_9^{2-}$ and $W_2Cl_9^{3-}$ lends credence to the exceptionally short W–W distance of 2.41 Å in the nonachloroditungstate(3–) dimer. A comparison of the moduli describing $Mo_2Cl_9^{3-}$ and $Mo_2Br_9^{3-}$ reveals the advantages of considering other factors in addition to the metal–metal distance in these structures. Even though the Mo–Mo separation increased by 0.16 Å when Br replaced Cl in the molybdenum dimers, the distortional parameters remained nearly unchanged for the two compounds. In the case of $W_2Br_9^{2-}$ and $W_2Cl_9^{3-}$ a difference in oxidation states exists in addition to the difference in the halogen ligands. Although the W–W distance differs by almost 0.19 Å between these two compounds, the distortional parameters indicate that the degree of contraction is nearly the same in both anions, so the variance in the metal–metal bond length can be attributed largely to the steric and electronic requirements of bridging Br atoms as compared to bridging Cl atoms.

The conclusion that steric requirements of the halide ligands dominate the metal–metal distance neglects the electron configuration difference between $W_2Br_9^{2-}$ and $W_2Cl_9^{3-}$. The formation of one σ and two π metal–metal bonding orbitals in confacial bioctahedrons has been cited previously in the literature.[1] A molecular orbital description of the bonding in a confacial bioctahedral dimer can be deduced by merging two octahedral monomers along a trigonal face. The assumption that the σ-bonding framework of the octahedral monomer remains basically intact allows one to energetically separate the nonbonding t_{2g} metal orbitals from the low-energy σ-bonding molecular orbitals which are filled with ligand electrons and the high-energy σ-antibonding molecular orbitals which are vacant. This leaves the partially filled metal t_{2g} orbitals (in O_h symmetry) to interact and form a total of six molecular orbitals in the D_{3h} dimer. As noted by Saillant and Wentworth,[10] the overlap between these metal d orbitals will produce a σ bonding molecular orbital of a_1' symmetry with an a_2'' antibonding mate and a degenerate set of e' π-bonding orbitals accompanied by an e'' antibonding set. The a_1' combination has no nodes and is doubtless the orbital of lowest energy among these six. One nodal plane is present in each of the e' orbitals but the overlap between the two metals is constructive, and these orbital energies will be lowered relative to the initial energies of the uncombined orbitals to provide metal–metal π bonding. The six valence d electrons available from the two metal atoms in $W_2Cl_9^{3-}$ are predicted to nicely fill the a_1' and degenerate e' bonding orbitals, hence producing a formal metal–metal bond order or 3. The $W_2Br_9^{2-}$ anion has five electrons available for metal–metal bonding, and consequently a bond order of 2.5 results since only three electrons occupy the e' orbitals. The contribution of a single electron in the π-bonding molecular orbitals may be a relatively minor force in determining the actual metal atom separation. Examining the results of comparing $Mo_2Cl_9^{3-}$ and $Mo_2Br_9^{3-}$ in light of a similar comparison between $W_2Cl_9^{3-}$ and $W_2Br_9^{2-}$ guides one toward such a conclusion. The 0.19 Å elongation of the W–W distance observed in $W_2Br_9^{2-}$ relative to $W_2Cl_9^{3-}$ is only 0.03 Å longer than the difference in the two $Mo_2X_9^{3-}$ (X = Cl, Br) dimers where the electron configuration remains unchanged.

Table VI. Distances and Angles Relevant to the Observed Distortion of $W_2Br_9^{2-}$ from D_{3h} Symmetry

Distances			
Br(7)–Br(8)–Br(9) Plane to Atom, Å			
Br(1)	2.66	Br(4)	2.87
Br(2)	2.84	Br(5)	2.68
Br(3)	2.74	Br(6)	2.70
Angles			
Normal to Br(7)–Br(8)–Br(9) Plane, Deg			
Normal to Br(1)–Br(2)–Br(3)		2.9	
Normal to Br(4)–Br(5)–Br(6)		3.4	

An interesting aspect of the electronic structure predicted for a confacial bioctahedron with five electrons in metal–metal bonding molecular orbitals is the existence of a $^2E'$ ground state. This orbital degeneracy requires that some distortion occur in order to break the degeneracy in accord with the theorem of Jahn and Teller.[28] The task of distorting the structure to remove the e' degeneracy cannot be accomplished by varying the metal–metal separation. However, one can envision an angular distortion which would preferentially lower the energy of one of the two π-bonding molecular orbitals.

The search for a small angular distortion in the structure of $[(n\text{-}C_3H_7)_4N]_2[W_2Br_9]$ consistent with the relative importance of the e' molecular orbital occupancy was rewarded by the following observation to which chemical significance may be attached. The three planes used to define d' and d'' (see Figure 4) were assumed to be perpendicular to the metal–metal axis, and in the D_{3h} case these planes are necessarily parallel to one another and perpendicular to the threefold axis by symmetry. Crystallographic threefold symmetry is not imposed on the $W_2Br_9^{2-}$ anion, however, and, in fact, the location of each of the 11 heavy atoms is independent of any symmetry restrictions. The distortion which is experimentally observed is a slight canting of the two planes defined by the two sets of three terminal bromine atoms toward the bridgehead position occupied by Br(8). Distances and angles relevant to this distortion are presented in Table VI.

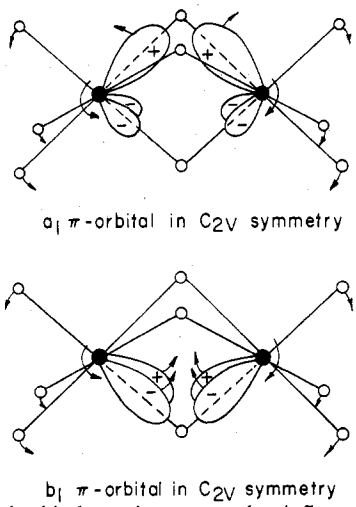

Figure 5. Metal orbital rotation proposed to influence the energy of the metal–metal π bonds.

This angular rotation by 3° of the terminal trigonal face of ligands on each tungsten atom may at first appear unrelated to the metal–metal π-bonding interaction. However, it is contended here that a strong link exists between the orientation of the d-orbital lobes used for metal–metal overlap and the spatial disposition of the remaining metal atom orbitals which form σ bonds to the ligands. It becomes evident upon examining the overlap considerations depicted in Figure 5 that a small rotation of the atomic orbitals on both tungsten atoms around axes perpendicular to the plane of the paper will effect the desired energy separation of the two e′ orbitals. The orbital rotation illustrated would increase the overlap of the b_1 π orbital, where the b_1 representation is appropriate after tilting the terminal ligand planes removes the C_3 axis and reduces the symmetry to C_{2v}. The overlap of the a_1 orbital which results from the second e′ molecular orbital due to the reduction in symmetry is decreased and hence the energy of this π orbital increases.

One could expect the union of two octahedra to form the dimeric $W_2Br_9^{2-}$ anion would fit in the category of negligible distortions since the odd electron is found in a "modified t_{2g} orbital", but an unknown perturbation is introduced by the metal–metal bonding. A subtle distortion that will favorably influence one of the two metal–metal π-bonding orbitals without altering metal–ligand bond strengths seems to be a likely result of the contributing factors. The complete absence of any detectable distortion could have been rationalized on the basis of comparisons with certain octahedral species for which Jahn–Teller distortions are predicted but not observed in crystal structures.

The point to be stressed is that there does exist a significant deviation from D_{3h} symmetry relative to the standard deviations for the parameters involved in the structure of $W_2Br_9^{2-}$. The distortion observed is real though small and is not observed in any of the other anions listed in Table V, with the exception of $Mo_2Cl_8H^{3-}$ which inherently has lower symmetry. Thus a chemical explanation can justifiably be sought. A survey of the nearest neighbor distances between the cations and the anion reveal no carbon–bromine separations of less than 3.80 Å and only seven heavy atom–light atom separations in the range of 3.80–4.00 Å. These distances are acceptable nonbonding separations with no systematic structural implications and thus are unlikely to cause the distortion observed in the dianion. Also, the center of the dianion resides at a general position in the cell indicating that any distortion caused by packing effects would not be of the symmetric type observed. Even the large thermal parameters observed for the cation are consistent with very weak interactions between cations and anions. Examination of nonbonded contacts within the $W_2Br_9^{2-}$ anion is not suggestive of violation of the van der Waals radii boundaries appropriate for bromide ligands. However, a close inspection of these distances (Table III) does reveal some trends which are small but significant in that they oppose the observed canted deformation rather than promote any tilt of the terminal ligand planes. On this basis it seems logical to discount steric hindrance among the bromide ligands as a possible contributor to the observed canted structure. On the contrary, to the extent that nonbonded contacts are important they oppose the observed small rotation of the terminal ligand faces since greater repulsions result as four of the terminal atoms approach the Br(8) bridging atom more closely.

Since packing forces and steric repulsions appear unlikely to cause the observed distortion, an electronic explanation seems appropriate. Metal–ligand σ bonds are not expected to favor any deviation from the idealized confacial bioctahedron. The a_1' metal–metal σ bond is axially symmetric and not influenced by angular distortions. This process of elimination leads one to the metal–metal π-orbital arena to explain the structural details.

That a slight rotation of the atomic orbitals on each of the tungsten atoms around an axis bisecting Br(7) and Br(1) on W(1) and bisecting Br(7) and Br(5) on W(2) would increase the overlap of the b_1 π orbital and decrease the overlap of the a_1 π orbital is clear from Figures 2 and 5. A combination of two angular displacements, with the orbitals on each tungsten atom rotated slightly, leads to an energy difference between the two π orbitals due to the overlap considerations discussed above. This orbital rotation mechanism is postulated as the route by which the e′ orbital degeneracy is broken in accord with the Jahn–Teller theorem. The actual orbital rotation which affects the metal–metal π-bonding orbitals is not directly observable, but the canted terminal ligand planes testify to the existence of this static angular deformation.

Acknowledgment. This work was supported by the U.S. Department of Energy, Division of Basic Energy Sciences.

Registry No. $[(n\text{-}C_3H_7)_4N]_2[W_2Br_9]$, 60318-96-9; $[(n\text{-}C_3H_7)_4N][W(CO)_2Br]$, 64314-95-0; $C_2H_4Br_2$, 106-93-4; $[(n\text{-}C_3H_7)_4N][Br]$, 1941-30-6; $W(CO)_6$, 14040-11-0.

Supplementary Material Available: Table of structure factors (11 pages). Ordering information is given on any current masthead page.

References and Notes

(1) F. A. Cotton and D. A. Ucko, *Inorg. Chim. Acta*, **6**, 161 (1972).
(2) O. Olsson, *Z. Anorg. Allg. Chem.*, **88**, 49 (1914).
(3) R. A. Laudise and R. C. Young, *Inorg. Synth.*, **6**, 149 (1960).
(4) E. A. Heintz, *Inorg. Synth.*, **7**, 142 (1963).
(5) R. Saillant, J. L. Hayden, and R. A. D. Wentworth, *Inorg. Chem.*, **6**, 1497 (1967).
(6) W. H. Watson and J. Waser, *Acta Crystallogr.*, **11**, 689 (1958).
(7) R. Saillant, R. B. Jackson, W. E. Streib, K. Folting, and R. A. D. Wentworth, *Inorg. Chem.*, **10**, 1453 (1971).
(8) R. C. Young, *J. Am. Chem. Soc.*, **54**, 4515 (1932).
(9) J. L. Hayden and R. A. D. Wentworth, *J. Am. Chem. Soc.*, **90**, 5291 (1968).
(10) R. Saillant and R. A. D. Wentworth, *J. Am. Chem. Soc.*, **91**, 2174 (1969).
(11) W. H. Delphin and R. A. D. Wentworth, *J. Am. Chem. Soc.*, **95**, 7920 (1973).
(12) W. H. Delphin and R. A. D. Wentworth, *Inorg. Chem.*, **13**, 2037 (1974).
(13) W. H. Delphin, R. A. D. Wentworth, and M. C. Matson, *Inorg. Chem.*, **13**, 2552 (1974).
(14) W. H. Delphin and R. A. Wentworth, *Inorg. Chem.*, **12**, 1914 (1973).
(15) E. W. Abel, I. S. Butler, and J. G. Reid, *J. Chem. Soc.*, 2068 (1963).
(16) J. G. Converse, Ph.D. Thesis, Iowa State University of Science and Technology, Ames, Iowa, 1968.
(17) R. A. Jacobson, *J. Appl. Crystallogr.*, **9**, 115 (1976).
(18) S. L. Lawton and R. A. Jacobson, *Inorg. Chem.*, **7**, 2124 (1968).
(19) R. A. Jacobson, J. A. Wunderlich, and W. N. Lipscomb, *Acta Crystallogr.*, **14**, 598 (1961).
(20) W. R. Busing, K. O. Martin, and H. A. Levy, "ORFLS, a Fortran Crystallographic Least Squares Program", U.S. Atomic Energy Commission Report ORNL-TM-305, Oak Ridge National Laboratory, Oak Ridge, Tenn., 1962.
(21) C. R. Hubbard, C. O. Quicksall, and R. A. Jacobson, "The Fast Fourier Algorithm and the Programs ALFF, ALFFDP, ALFFPROJ, ALFFT, and FRIEDEL", U.S. Atomic Energy Commission Report IS-2625, Iowa

State University and Institute for Atomic Research, Ames, Iowa, 1971.
(22) H. P. Hanson, F. Herman, J. D. Lea, and S. Skillman, *Acta Crystallogr.*, **17**, 1040 (1964).
(23) D. H. Templeton in "International Tables for X-Ray Crystallography", Vol. III, Kynoch Press, Birmingham, England, 1962, pp 215–216.
(24) W. R. Busing, K. O. Martin, and H. A. Levy, "ORFFE, a Fortran Crystallographic Function and Error, Program", U.S. Atomic Energy Commission Report ORNL-TM-306, Oak Ridge National Laboratory, Oak Ridge, Tenn., 1964.
(25) J. E. Fergusson in "Preparative Inorganic Reactions", Vol. 7, W. L. Jolly, Ed., Wiley-Interscience, New York, N.Y., 1971, pp 93–163.
(26) E. T. Maas, Jr., and R. E. McCarley, *Inorg. Chem.*, **12**, 1096 (1973).
(27) R. J. Ziegler and W. M. Risen, *Inorg. Chem.*, **11**, 2796 (1972).
(28) H. Jahn and E. Teller, *Phys. Rev.*, **49**, 874 (1937).

Contribution from the Department of Chemistry, Emory University, Atlanta, Georgia 30322

Synthesis and Crystal Structure of (Dimethylthiocarboxamido)(dimethylamino[dimethyldithiocarbamato]carbene)nickel(II) Tetraphenylborate, $[Me_2NCSNiC(NMe_2)SC(NMe_2)S]BPh_4$, a Stable Nickel Carbene Complex

WALTER K. DEAN,* ROBERT S. CHARLES, and DONALD G. VANDERVEER

Received May 16, 1977 AIC70349K

The title compound $[Me_2NCSNiC(NMe_2)SC(NMe_2)S]BPh_4$ has been prepared by the direct reaction of dimethylthiocarbamoyl chloride with nickel carbonyl or with bis(cyclopentadienyl)nickel, followed by metathesis with $NaBPh_4$. The compound crystallizes in the monoclinic space group $P2_1/n$ with four formula units in a unit cell with dimensions $a = 9.208$ (2) Å, $b = 22.837$ (8) Å, $c = 15.823$ (5) Å, and $\beta = 99.01$ (2)°. Full-matrix least-squares refinement of 2496 independent counter data yielded a final unweighted R factor of 0.074. The planar cation contains a chelating thiocarboximido group and a (dimethylamino)dimethyldithiocarbamatocarbene ligand in which the dithiocarbamato group is coordinated to the nickel by one sulfur atom, forming a unique chelating carbene ligand. The structural features of this complex are discussed and compared with those of related compounds. The two nickel–carbon distances are 1.854 (11) Å (to the thiocarboxamido group) and 1.909 (10) Å (to the carbene ligand); there appears to be no indication of substantial π interaction between the nickel atom and the carbenoid carbon atoms in this compound.

Introduction

In previous papers we have reported reactions of dimethylthiocarbamoyl chloride with metal carbonyl anions,[1] and recently we have extended these investigations to include reactions of this versatile reagent with neutral metal carbonyls as well.[2] These reactions yield a variety of metal complexes containing dithiocarbamate ligands, chelating and bridging thiocarboxamido groups, and various exotic carbene ligands.

In this paper we report the reaction of dimethylthiocarbamoyl chloride with nickel tetracarbonyl or nickelocene to give complexes initially formulated as $[Ni(CSNMe_2)_3]X$ ($X^- = Cl^-$, PF_6^-, BPh_4^-). These products are isolated as orange, diamagnetic solids which are stable indefinitely in air. Their NMR spectra show all methyl groups to be nonequivalent, and no clues to their structure were provided by other spectroscopic methods. Accordingly a crystal structure study was undertaken of the tetraphenylborate salt with a view to its structural characterization. The results of this study, along with an account of the syntheses of the complexes, are reported here.

Experimental Section

Synthesis of the Complexes. All reagents were obtained from commercial sources. Dimethylthiocarbamoyl chloride ($ClCSNMe_2$) was recrystallized from diethyl ether before use. Tetrahydrofuran was distilled from calcium hydride. All operations were performed under a nitrogen atmosphere.

Infrared spectra were recorded on a Perkin-Elmer 467 spectrophotometer. Proton NMR measurements were made with a Jeol JNM-MH-100 instrument. Analyses were performed by the Atlantic Microanalytical Laboratories, Atlanta, Ga.

Reaction of Nickel Carbonyl with $ClCSN(CH_3)_2$. $Ni(CO)_4$ (1.00 g, 5.85 mmol) and $ClCSNMe_2$ (2.17 g, 17.6 mmol) were stirred in 50 mL of tetrahydrofuran. Evolution of CO was observed and the product separated as an orange precipitate. After 18 h the reaction was complete; the mixture was diluted with 100 mL of diethyl ether, stirred for 1 h, and filtered, yielding 1.23 g (3.42 mmol, 58.4%) of $[Me_2NCSNiC(NMe_2)SC(NMe_2)S]Cl$.

The same compound was obtained in 48.5% yield by the reaction of bis(cyclopentadienyl)nickel with $ClCSNMe_2$ under the same conditions.

Because the chloride was rather hygroscopic, it was converted quantitatively into the hexafluorophosphate or tetraphenylborate (by treatment with aqueous NH_4PF_6 or $NaBPh_4$) before analysis.

Analytical, NMR, and infrared data on these compounds are given in Table I.

Collection of X-Ray Diffraction Data. Suitable crystals of $[Me_2NCSNiC(NMe_2)SC(NMe_2)S]BPh_4$ were obtained by slow cooling of an acetone solution of the salt. Crystals were mounted on glass fibers with epoxy cement. Examination of preliminary Weissenberg and precession photographs showed systematic absences ($0k0$, $k = 2n + 1$; $h0l$, $h + l = 2n + 1$) indicating space group $P2_1/n$, a nonstandard setting of space group $P2_1/c$ which was maintained throughout the structure solution and refinement because of the near orthogonality of the axes.

Intensity data were collected on a Syntex $P2_1$ automated four-circle diffractometer equipped with a graphite monochromator. The data were corrected for Lorentz and polarization effects, using the form of the Lp factor given in eq 1. (This equation assumes that the

$$Lp = \frac{0.5}{\sin 2\theta}\left[\left(\frac{1 + \cos^2 2\theta_m \cos^2 2\theta}{1 + \cos^2 2\theta_m}\right) + \left(\frac{1 + |\cos 2\theta_m| \cos^2 2\theta}{1 + |\cos 2\theta_m|}\right)\right] \quad (1)$$

graphite monochromator crystal is 50% perfect and 50% mosaic; the monochromator angle $2\theta_m$ is 12.2° for Mo Kα radiation.)

Standard deviations $\sigma(I)$ were estimated by the procedure of Doedens and Ibers,[3] using an "ignorance factor" of 0.05. No corrections were made for absorption.

Because the first crystal diffracted weakly, giving an abnormally high percentage of unobserved reflections, a second data set was collected using a different crystal. The two sets were of comparable quality and were correlated before the final refinement. A total of